The following publication Y. Jiang, Y. Yang, S. -C. Tan and S. -Y. R. Hui, "Mitigating Distribution Power Losses of Standalone AC Microgrids Using Particle-Swarm-Optimization Control for Distributed Battery Systems," 2019 IEEE Applied Power Electronics Conference and Exposition (APEC), 2019, pp. 3224-3229 is available at https://doi.org/10.1109/APEC.2019.8721988

Mitigating Distribution Power Losses of Standalone AC Microgrids Using Particle-Swarm-Optimization Control for Distributed Battery Systems

Yajie Jiang*, Yun Yang*, Siew-Chong Tan*, and Shu-Yuen Ron Hui*†

*Department of Electrical and Electronic Engineering, The University of Hong Kong, Hong Kong, China
†Department of Electrical and Electronic Engineering, Imperial College London, London, U.K.
Email: yjjiang@eee.hku.hk, cacaloto@hku.hk, sctan@eee.hku.hk, ronhui@eee.hku.hk.

***Abstract*—Distributed battery systems (DBS) are widely used in microgrids to compensate imbalanced active and reactive power flows, and for stabilizing bus voltages of microgrids with a high penetration of renewable energy sources (RES). In this paper, a particle-swarm-optimization (PSO) method is adopted as the secondary control of DBS in a standalone AC microgrid. The fitness function of the PSO algorithm contains the parameters of the bus voltage deviations and the power losses on the distribution lines. Through iteration, the bus voltage deviations and the power losses on the distribution lines are reduced, simultaneously. Importantly, the State-of-Charges (SOC) of the battery packs are also being taken into consideration and the battery packs are controlled by local controllers to prevent deep-discharge and over-charge. Both results from Matlab simulation and Real-Time Digital Simulator (RTDS) validate the effectiveness of the proposed control scheme in concurrently reducing the distribution power losses and meeting bus voltage regulations in AC microgrids.**

***Index Terms*—AC microgrid, bus voltage regulation, distribution power losses, particle-swarm-optimization (PSO).**

I. Introduction

Microgrids comprising renewable energy sources (RES), energy storage systems (ESS), various types of loads, and power electronic interfaces have been widely investigated by different researchers [1]-[4]. The use of standalone microgrids, which is a popular trend for data centers' application, can suffer from serious power imbalance and bus voltage fluctuations caused by intermittent RES [5], [6]. ESS, such as batteries, super-capacitors, and flywheels have to be introduced to compensate both the active and reactive power imbalances to alleviate bus voltage fluctuations [7]–[9].

Thereinto, due to their high energy densities and relatively simple control, batteries have been the most widely used ESS for such applications [10]. As the batteries are usually distributedly installed over the microgrids, they are known as distributed battery systems (DBS). Conventionally, the droop control or modified droop control are adopted as the primary control in DBS/RES for regulating the bus voltages. So far, different strategies have been proposed. In [11], a scheme involving a voltage compensation term that is proportional to the integration of the active power is proposed to achieve bus voltage restoration. In [12], an integral-droop combined controller is adopted to improve the power quality of an AC microgrid. In [13], a combination of virtual inductance method and frequency droop control is introduced to damp the power oscillation. In [14], an interlinking control scheme is presented to balance the active power in a hybrid microgrid. In [15], a multi-agent flow strategy is proposed to optimize the dynamic power flow in a microgrid, which further enhances the power quality. In [16], based on the average voltage deviation, a secondary frequency and voltage control method is applied in an islanded microgrid to simultaneously achieve critical bus voltage tracking and accurate reactive power sharing. In [17], a consensus algorithm is adopted to set the voltage reference of a RES node based on the measurement of neighboring RES nodes to achieve good bus voltage tracking capability. In [18], a centralized model predictive control is proposed to regulate the bus voltages of DC electric springs to mitigate the distribution power losses of a DC microgrid while meeting voltage regulation standards. So far, there are relatively few works that report and take into consideration the power losses on the distribution lines as a control parameter.

Swarm intelligence algorithms are well-established technique that can deal with complex optimization problems without knowing specific parameters of the system. Thereinto, particle-swarm-optimization (PSO) is a heuristic algorithm that has been applied to power systems to optimize the economic profits [19]-[21], the power dispatch [22], [23], and the power quality [24]-[26]. PSO possesses the merits of high accuracy, strong reliability, and fast convergence speed in optimizing the parameters of multivariate coupling systems.

In this paper, a PSO-based control strategy is developed for DBS to concurrently regulate the bus voltages of a microgrid and state-of-charges (SOC) of the batteries, while mitigating the power losses on the distribution lines. In the process, the bus voltages, line currents, and SOC of the DBS are measured as feedbacks to the fitness function of the proposed control strategy. Consequently, optimal bus voltage references for the DBS can be searched using several iterations within the constraints of the bus voltages and the SOC of the batteries. Verification works are carried out in the Matlab platform and by using a Real-Time Digital Simulator (RTDS).

II. Overview of the Proposed Control Strategy

A typical architecture of a standalone AC microgrid is shown in Fig. 1. The microgrid comprises several RES units, loads, DBS, and power electronics interfaces. The DBS are adopted to compensate both active and reactive power flows. When the supplied power by the RES is excessive relative to the grid demand, the DBS will operate in the charge mode. Conversely, when the supplied power by the RES is insufficient relative to the grid demand, the DBS operate in the

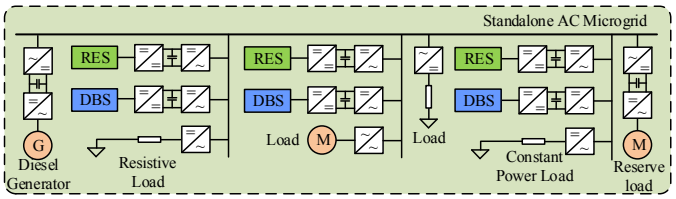

Fig. 1. A typical architecture of a standalone AC microgrid.

discharge mode. Besides, to prolong the lifespan of the batteries (by preventing it from entering deep-discharge), the diesel generators will be activated to operate once the SOC of the DBS are lower than a specified lower limit. Conversely, in the charge mode, the reserve loads will be activated to operate once the SOC of the DBS are higher than a specified upper limit. This prevents the DBS from going into an over-charge.

The flowchart of the control strategy for the DBS is shown in Fig. 2. In the figure, r, v_{br} and i_{br} represent the battery number, voltage and output current of the battery, respectively. V_{busa} is the measured line bus voltage, I_{ab} is the root-mean-square (RMS) value of the current between bus a and bus b, and V_{refr}^{*} is the bus voltage reference from the PSO control. Here, the values of SOC are estimated using

$$\mathrm{SOC}_r = \mathrm{SOC}_r(0) - \frac{1}{C_{er}}\int i_{br}\,dt \tag{1}$$

where $\mathrm{SOC}_r(0)$ and C_{er} are the initial SOC and the capacity of the battery unit r, respectively.

III. Proposed PSO Control for DBS

The PSO control provides the optimal line bus voltage reference values V_{refr}^{*} for the local controllers. The flowchart of the PSO control is shown in Fig. 3. An explanation of the flow of the control strategy is given as follow.

Step 1: Initialization

Initialize the parameters of the inertia weight w, the velocity v, the position x_i, the learning factors c_1 and c_2, and the population size G. Generate the random initial positions x_i within the search range as

$$x_i = V_{\min} + rand(V_{\max} - V_{\min}) \tag{2}$$

where i is the number of the particles; V_{nom} is the nominal line bus voltage; and $V_{\max}$ and $V_{\min}$ are the upper limit and the lower limit of the line bus voltage, respectively.

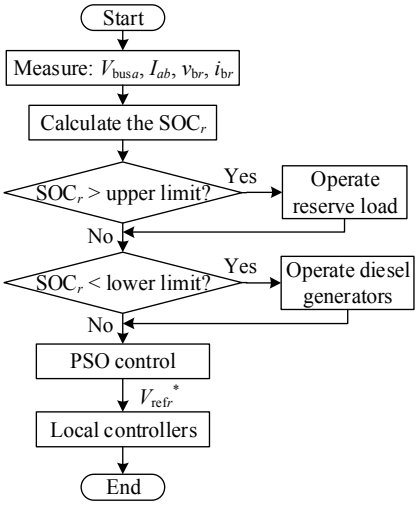

Fig. 2. Control strategy for the DBSs.

Step 2: Fitness Function Calculation

The fitness function of the PSO control is

$$J = \alpha\sum_{a=1}^{m}\left|V_{\mathrm{nom}} - V_{busa}\right| + (1-\alpha)\sum_{a,b=1}^{m} I_{ab}^{2}R_{ab} \tag{3}$$

where m is the number of the buses; α is the weighting factor; and R_{ab} is the resistance between bus a and bus b. The fitness function includes parameters of both the bus voltage deviations and the line losses.

Step 3: Update of Inertia Weight, Velocity, and Position

To accelerate the global search, the drop function for the inertia weight is

$$w_i = w_{\max} - \frac{k*(w_{\max} - w_{\min})}{G} \tag{4}$$

where k is the number of iterations of the PSO control, and $w_{\max}$ and $w_{\min}$ are the tolerances of the inertia weight. Then, the equations of the updated velocity and position are given as

$$\begin{aligned} v_i^{k+1} &= w_i v_i^k + c_1 * rand(p_{besti} - x_i^k) + c_2 * rand(g_{\mathrm{best}} - x_i^k) \\ x_i^{k+1} &= x_i^k + v_i^{k+1} \end{aligned} \tag{5}$$

where p_{besti} is the best position of the i_{th} particle and g_{best} is the best position of the population. Certainly, all the positions are limited by $V_{\min} \le x_i^{k+1} \le V_{\max}$.

Step 4: The Search for p_{besti}, g_{best}, J_{besti}, and J_{best}.

The selection process can be given as

for $i = 1:10$

if $J_i^k < J_{\mathrm{best}\,i}$ then $p_{\mathrm{best}\,i} = x_i^k$, $J_{\mathrm{best}\,i} = J_i^k$ endif (6)

if $J_{\mathrm{best}} < J_{\mathrm{best}\,i}$ then $g_{\mathrm{best}} = p_{\mathrm{best}\,i}$, $J_{\mathrm{best}} = J_{\mathrm{best}\,i}$ endif (7)

endfor

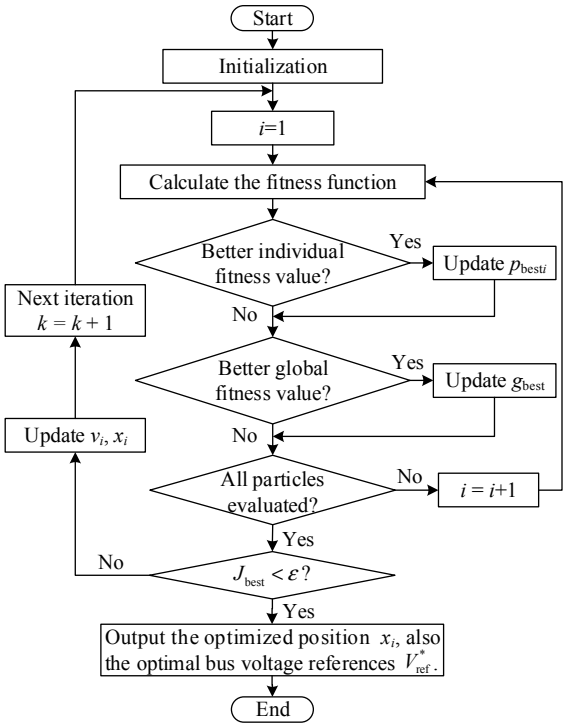

Fig. 3. Flowchart of the PSO control.

Step 5: Iteration of Search (Step 2 to 4) Till End

In case the stop-searching criterion $J_{best}<\varepsilon$ (ε is predefined) is satisfied, the PSO control stops the search and outputs the optimized positions, which are the optimal line bus voltage reference V^*_{refr} for the local controller. The schematic diagram of the proposed PSO control is shown in Fig. 4.

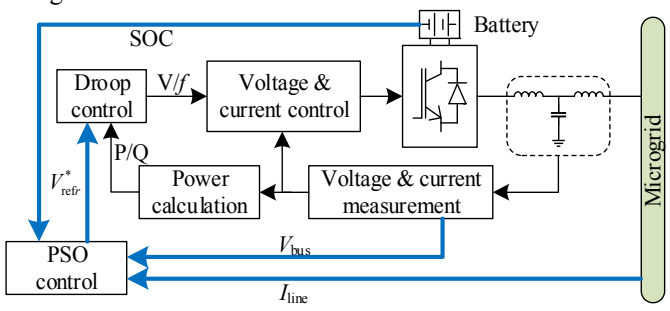

Fig. 4. Schematic diagram of the proposed PSO control.

IV. Simulation Results

To verify the performance of the proposed PSO control, simulation of a five-bus AC microgrid is carried out in Matlab/Simulink. The topology of the five-bus microgrid is shown in Fig. 5. Here, two RES are installed at Bus 2 and Bus 4, respectively. The diesel generator is installed at Bus 1. Reserve loads are installed at Bus 5. All buses are load-connected. The parameters of the microgrid and the PSO control strategy are given in Table I and II, respectively.

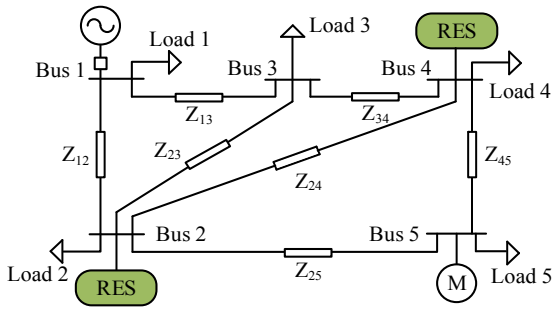

Fig. 5. Topology of the five-bus microgrid.

TABLE I. Parameters of the Five-Bus Microgrid

Parameters	Value
Nominal voltage (V_{nom})	380 V
Nominal frequency (f)	50 Hz
Load 1 (S_1)	1000 W + 200 VAR
Load 2 (S_2)	2000 W + 200 VAR
Impedance of Load 3 (Z_3)	100 Ω + 1 μH
Load 4 (S_4)	2000 W + 600 VAR
Load 5 (S_5)	1000 W + 200 VAR
Line resistance between Bus 1 and 2 (R_{12})	1.2730 Ω
Line resistance between Bus 1 and 3 (R_{13})	0.6365 Ω
Line resistance between Bus 2 and 3 (R_{23})	0.7638 Ω
Line resistance between Bus 2 and 4 (R_{24})	0.7638 Ω
Line resistance between Bus 2 and 5 (R_{25})	1.5276 Ω
Line resistance between Bus 3 and 4 (R_{34})	1.0184 Ω
Line resistance between Bus 4 and 3 (R_{45})	1.2730 Ω

TABLE II. Parameters of the Proposed PSO Control

Parameters	Value
Execution cycle (T_{pso})	0.05 s
Population size (G)	10
Local learning factor (c_1)	1.3
Global learning factor (c_2)	1.7
Upper limit of inertia weight (w_{max})	0.9
Lower limit of inertia weight (w_{min})	0.1
Upper limit of velocity (v_{max})	2.0 V
Lower limit of velocity (v_{min})	–2.0 V
Upper limit of position/voltage (V_{max})	399 V
Lower limit of position/voltage (V_{min})	361 V

A. Case Studies with Fixed Weighting Factors

The waveforms of the bus voltages (RMS), voltage references (RMS), and the fitness values for three cases with a fixed weighting factor of 0.9 are given in Figs. 6 to 8, respectively. The PSO control is activated at time = 6 s. In the searching period, the bus voltages fluctuate. The optimal voltage references are obtained as V_{ref4}=396.4 V for Case 1, V_{ref4}=397.8 V and V_{ref5}=382.2 V for Case 2, and V_{ref1}=381.5 V, V_{ref4}=384.4 V, and V_{ref5}=381.4 V for Case 3. Clearly, the bus voltage tracking performances are improved, and the distribution power losses are mitigated when more DBS are installed in the microgrid. And the searching periods of the PSO are longer for more DBS installed in the microgrid.

Figs. 9 and 10 present the comparisons of the distribution power losses and voltage tracking errors between the DBS with conventional droop control and that with the proposed PSO control. With the PSO control, the distribution power losses are mitigated by 1.14% in Case 1, 1.42% in Case 2, and 2.48% in Case 3, as compared to that with conventional control. Meanwhile, the bus voltage deviations are reduced by 6.51% in Case 1, 9.56% in Case 2, and 15.32% in Case 3, respectively. Apparently, with more DBS installed in the microgrid, both the distribution power losses and the bus voltage deviations are reduced.

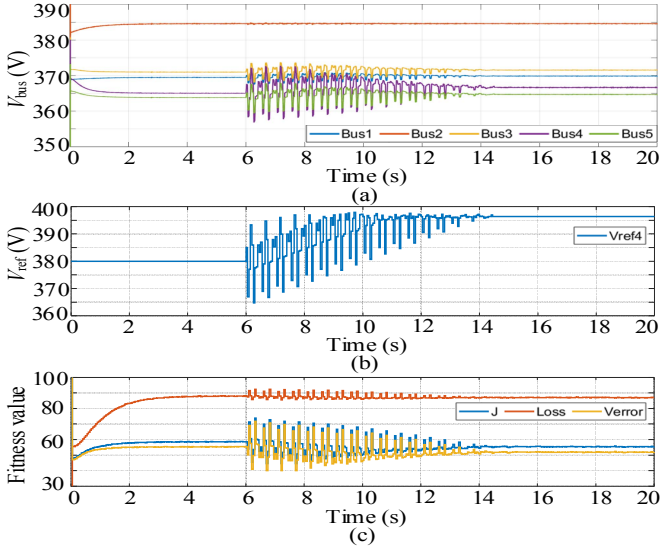

Fig. 6. Case 1: (a) bus voltages (RMS), (b) bus voltage reference (RMS), and (c) fitness values of the DBS at Bus 4 with α=0.9.

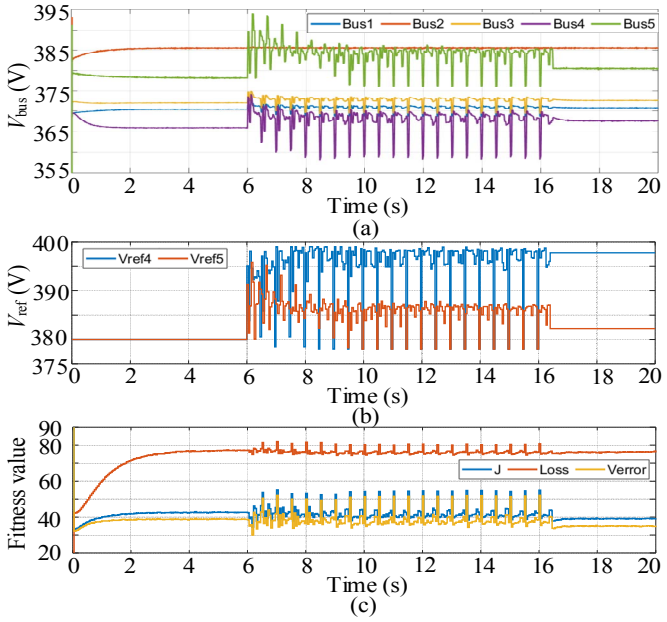

Fig. 7. Case 2: (a) bus voltages (RMS), (b) bus voltage references (RMS), and (c) fitness values of the DBS at Bus 4 and 5 with α=0.9.

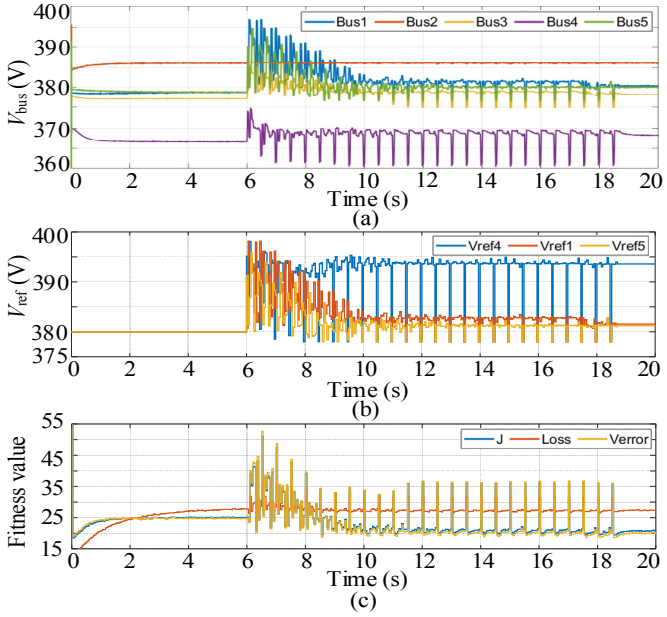

Fig. 8. Case 3: (a) bus voltages (RMS), (b) bus voltage references (RMS), and (c) fitness values of the DBS at Bus 1, 4, and 5 with α=0.9.

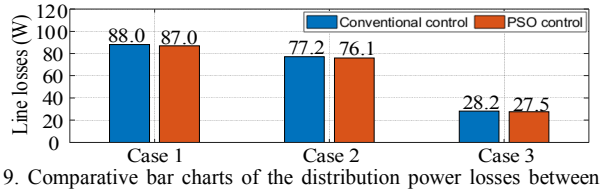

Fig. 9. Comparative bar charts of the distribution power losses between the DBS with conventional droop control and that with the proposed PSO control.

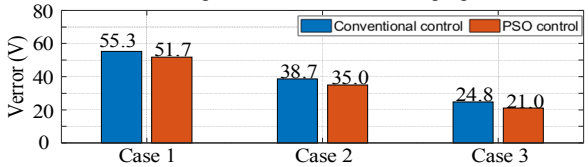

Fig. 10. Comparative bar charts of the voltage tracking errors between the DBS with conventional droop control and that with the proposed PSO control.

B. Case Studies with Variable Weighting Factors

The weighting factor of the fitness function affects the bus voltage tracking performance and the power losses on the distribution lines. Theoretically, a greater value of the weighting factor α results in better bus voltage tracking performance and higher distribution power losses. In these case studies with variable weighting factors, the PSO control are used for the DBS at Bus 2 and Bus 4 with α=0.9, α=0.15, and α=0.09, respectively. The results are shown in Figs. 11 to 13. Clearly, the bus voltage tracking performances obtained in Fig. 11 is better than that in Fig. 12, which is better than that in Fig. 13. Conversely, the distribution power losses obtained in Fig. 13 is less than that shown in Fig. 11 and Fig. 12. The optimal voltage references are V_{ref2}=394.3 V and V_{ref4}=395.7 V for Case 4, V_{ref2}=376.85 V and V_{ref4}=394.2 V for Case 5, and V_{ref2}=366.35 V and V_{ref4}=393.83 V for Case 6.

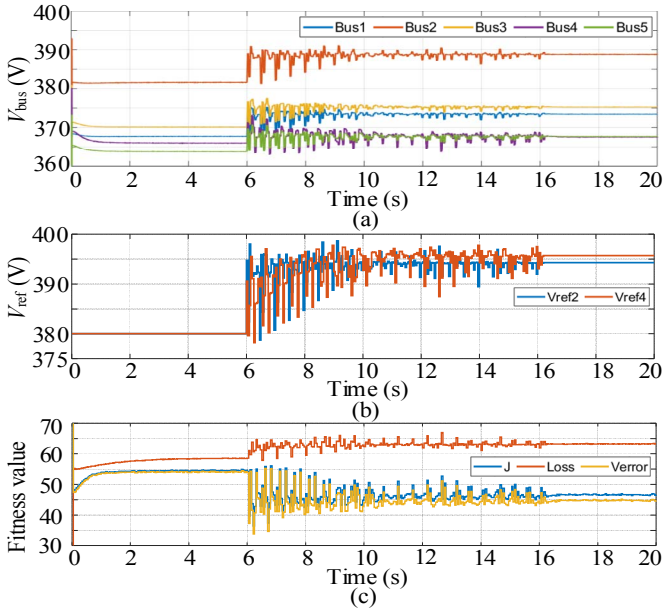

Fig. 11. Case 4: (a) bus voltages (RMS), (b) bus voltage references (RMS), and (c) fitness values of the DBS at Bus 2 and 4 with α=0.9.

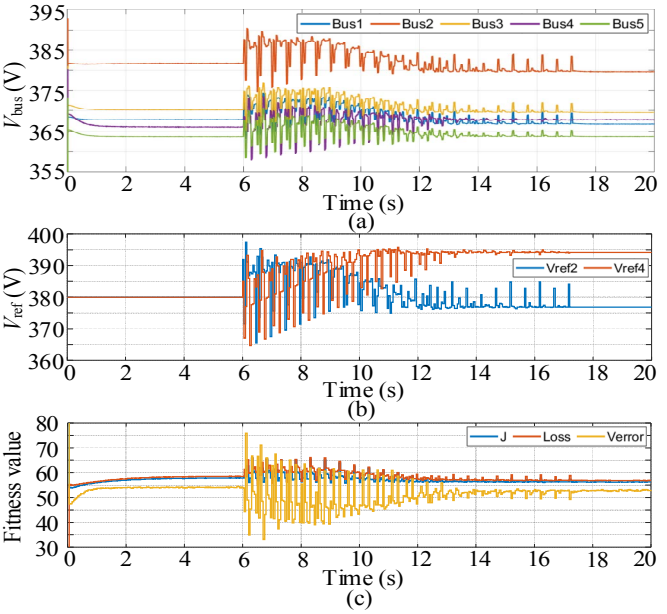

Fig. 12. Case 5: (a) bus voltages (RMS), (b) bus voltage references (RMS), and (c) fitness values of the DBS at Bus 2 and 4 with α=0.15.

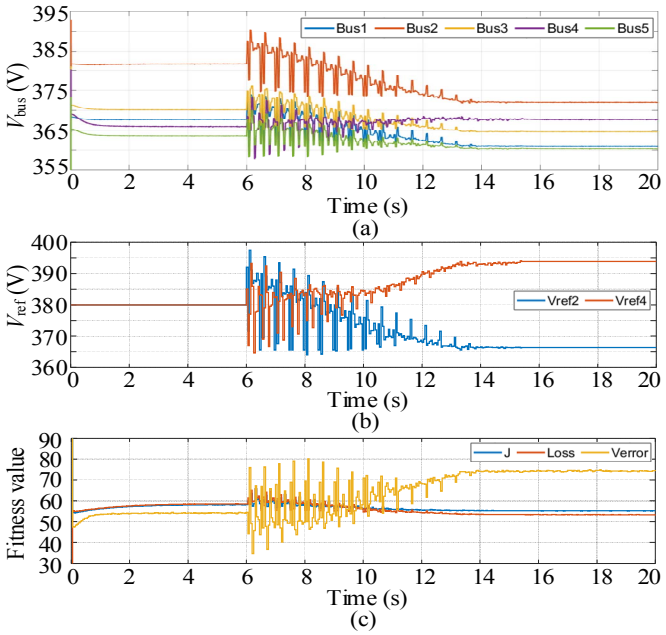

Fig. 13. Case 6: (a) bus voltages (RMS), (b) bus voltage references (RMS), and (c) fitness values of the DBS at Bus 2 and 4 with α=0.09.

Fig. 14 gives a comparison of the distribution power losses and bus voltage deviations of the system among the different weighting factors. Apparently, the distribution power losses on the microgrid decrease while the bus voltage deviations increase as weighting factor is set smaller. With the proposed PSO control, the bus voltage deviations are reduced by about 19.44% in Case 4, and the distribution power losses are mitigated by about 9.04% in Case 6, as compared to that with conventional control. Importantly, both objectives of mitigating distribution power losses and bus voltage deviations can be optimally balanced, as shown in Case 5.

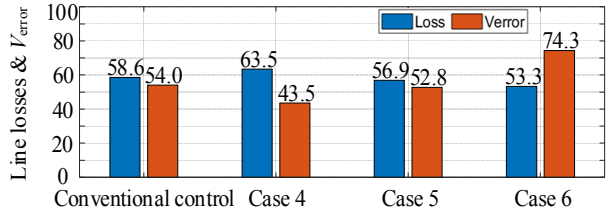

Fig. 14. Comparative bar charts of the distribution power losses and bus voltage deviations among the PSO control with different weight factors.

Fig. 15 shows the plots of the real-time SOC of the DBS installed at Bus 2 and 4 for Case 5 (SOC2 indicates the SOC of the battery pack at Bus 2 and SOC4 indicates the SOC of the battery pack at Bus4). Initially, as the power supplied by the RES is insufficient in meeting the demand, both DBS operate in discharge mode. When SOC2 reaches 20%, DBS2 stops discharging but the DBS4 continues to discharge until SOC4 reaches 20%. At that instance, as the power supplied by the RES is still falling short of the demand, the diesel generator operates to compensate the shortfall power. When power supplied by the RES is in surplus, the diesel generator goes into idling mode and the DBS starts to charge. When the SOC of both DBS reach 90% and the power supplied by the RES are still having a surplus, the reserve loads activate to consume the redundant power. When the supplied power by the RES fall short, the reserve loads are disconnected and the DBS start to discharge.

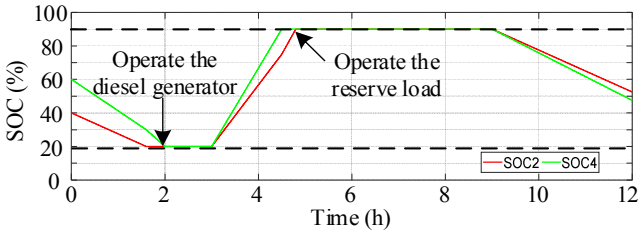

Fig. 15. SOC of the DBS at Bus 2 and 4 with the proposed PSO control.

The bus voltages (RMS) of the microgrid with the conventional droop control and that with the proposed PSO control are listed in Table III and IV, respectively.

TABLE III
BUS VOLTAGES OF THE MICROGRID WITH THE CONVENTIONAL CONTROL

Case\Voltage	Bus 1	Bus 2	Bus 3	Bus 4	Bus 5
Case 1	369.4 V	384.7 V	371.0 V	365.0 V	363.9 V
Case 2	370.5 V	385.6 V	372.1 V	365.9 V	378.3 V
Case 3	378.8 V	386.2 V	377.2 V	366.6 V	378.8 V
Case 4,5,6	367.8 V	381.5 V	370.0 V	365.9 V	363.6 V

TABLE IV
BUS VOLTAGES OF THE MICROGRID WITH THE PROPOSED PSO CONTROL

Case\Voltage	Bus 1	Bus 2	Bus 3	Bus 4	Bus 5
Case 1	380.0 V	384.8 V	371.6 V	366.7 V	364.6 V
Case 2	370.8 V	385.5 V	372.5 V	367.6 V	380.4 V
Case 3	380.6 V	386.2 V	378.3 V	368.2 V	380.0 V
Case 4	373.4 V	388.9 V	375.3 V	367.5 V	367.6 V
Case 5	366.7 V	379.7 V	369.6 V	367.8 V	363.6 V
Case 6	361.0 V	372.1 V	364.6 V	367.7 V	360.4 V

V. RESULTS IN RTDS

The circuit model of the five-bus microgrid is built in RSCAD for Case 6 and tested using the RTDS. The steady-state waveforms of Bus 1 voltage and the waveforms of RMS values of the five buses of the microgrid with conventional control and that of the proposed PSO control are presented in Figs. 16 and 17. The comparisons of the bus voltage deviations and the distribution power losses between the conventional control and that of the proposed PSO control are given in Fig. 18. It is found that with the proposed PSO control, although the bus voltage deviations are increased, they are still regulated within the tolerance of ±5%. Accordingly, the distribution power losses are mitigated by about 5.46% as compared to that with conventional control.

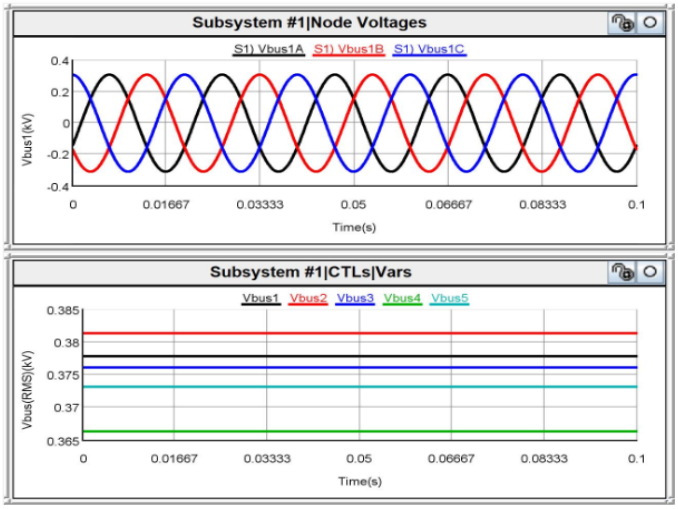

Fig. 16. Waveforms of the steady-state Bus 1 voltage and the bus voltages in RMS values with the conventional control.

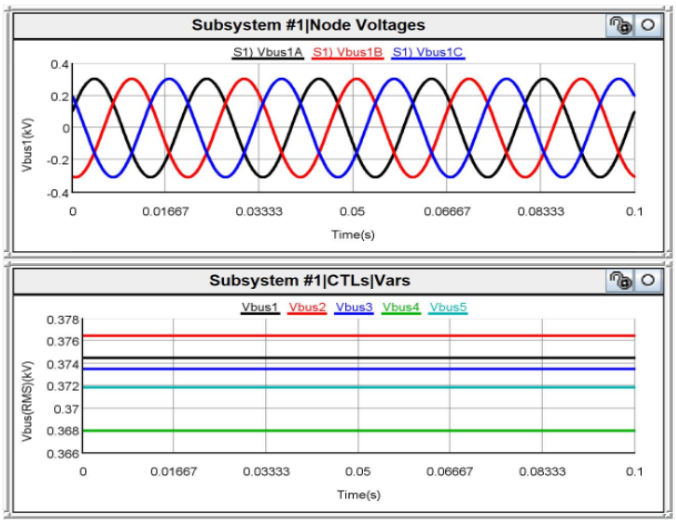

Fig. 17. Waveforms of the steady-state Bus 1 voltage and the bus voltages in RMS values with the proposed PSO control.

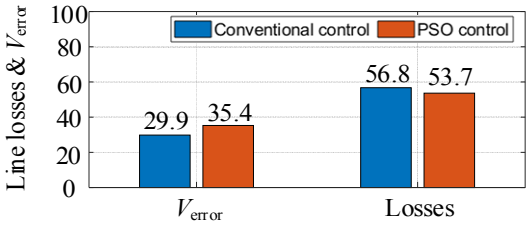

Fig. 18. Comparative bar charts of the bus voltage deviations and the distribution power losses between the conventional control and the proposed PSO control.

VI. Conclusions

Conventional droop control methods are widely used in distributed battery systems (DBS) to regulate the bus voltages and SOC of the batteries in standalone AC microgrids. In this paper, a particle-swarm-optimization (PSO) control is proposed to not only regulate the bus voltages and the SOC of the batteries, but also mitigate power losses on the distribution lines. The effectiveness of the proposed PSO control are demonstrated via various case studies in the Matlab and the Real-Time Digital Simulator (RTDS). The results obtained from the RTDS illustrate the distribution power losses of an AC microgrid with the proposed control can be mitigated by about 5.46% while the bus voltages are still regulated within the tolerance, as compared to that of the conventional control.

References

[1] J. Guerrero, P. Loh, T. Lee, and M. Chandorkar, "Advanced control architectures for intelligent microgrids—part II: power quality, energy storage, and AC/DC microgrids," *IEEE Trans. Ind. Electron.*, vol. 60, no. 4, pp. 1263-1270, Apr. 2013.

[2] D. Boroyevich, I. Cvetkovic, D. Dong, R. Burgos, W. Fei, and F. Lee, "Future electronic power distribution systems—A contemplative view," in *12th Int. Conf. Optim. Electr. Electron. Equip.*, 2010, pp. 1369-1380.

[3] A. Gupta, S. Doolla, and K. Chatterjee, "Hybrid AC–DC microgrid: systematic evaluation of control strategies," *IEEE Trans. Smart Grid*, vol. 9, no. 4, pp. 3830-3843, Jul. 2018.

[4] S. C. Tan, C. K. Lee, and S. Y. Hui, "General steady-state analysis and control principle of electric springs with active and reactive power compensations," *IEEE Trans. Power Electron.*, vol. 28, no. 8, pp. 3958-3969, Aug. 2013.

[5] S. Y. Hui, C. K. Lee, and F. F. Wu. "Electric springs—A new smart grid technology," *IEEE Trans. Smart Grid*, vol. 3, no. 3, pp. 1552-1561, Sept. 2012.

[6] Q. Jiang, Y. Gong, and H. Wang, "A battery energy storage system dual-layer control strategy for mitigating wind farm fluctuations," *IEEE Trans. Power Syst.*, vol. 28, no. 3, pp. 3263-3273, Aug. 2013.

[7] K. Zou, A. Agalgaonkar, K. Muttaqi, and S. Perera, "Distribution system planning with incorporating DG reactive capability and system uncertainties," *IEEE Trans. Sust. En.*, vol. 3, no. 1, pp. 112-123, 2011.

[8] D. Wu, F. Tang, T. Dragicevic, J. Vasquez, and J. Guerrero, "Autonomous active power control for islanded AC microgrids with photovoltaic generation and energy storage system," *IEEE Trans. Energy Convers.*, vol. 29, no. 4, pp. 882-892, Dec. 2014.

[9] H. Zhou, T. Bhattacharya. D. Tran, T. Siew, and A. Khambadkone, "Composite energy storage system involving battery and ultracapacitor with dynamic energy management in microgrid applications," *IEEE Trans. Power Electron.*, vol. 26, no. 3, pp. 923-930, Mar. 2011.

[10] C. Li, T. Dragicevic, J. C. Vasquez, *et al.*, "Multi-agent-based distributed state of charge balancing control for distributed energy storage units in AC microgrids," in *Proc. 2015 IEEE Appl. Power Electron. Conf. Expo., Charlotte, NC, USA*, 2015, pp. 2967-2973.

[11] X. Sun, Y. Hao, Q. Wu, X. Guo, and B. Wang, "A multifunctional and wireless droop control for distributed Eenergy storage units in islanded AC microgrid applications," *IEEE Trans. Power Electron.*, vol. 32, no. 1, pp. 736-751, Jan. 2017.

[12] J. Kim, J. Guerrero, *et al.* "Mode adaptive droop control with virtual output impedances for an inverter-based flexible AC microgrid," *IEEE Trans. Power Electron.*, vol. 26, no. 3, pp. 689-701, Mar. 2011.

[13] Y. Sun, X. Hou, J. Yang, H. Han, M. Su, and J. M. Guerrero, "New perspectives on droop control in AC microgrid," *IEEE Trans. Ind. Electron.*, vol. 64, no. 7, pp. 5741-5745, Jul. 2017.

[14] P. C. Loh, D. Li, Y. K. Chai, and F. Blaabjerg, "Autonomous control of interlinking converter with energy storage in hybrid AC–DC microgrid," *IEEE Trans. Ind. Appl.*, vol. 49, no. 3, pp. 1374-1382, May 2013.

[15] T. Morstyn, B. Hredzak, and V. G. Agelidis, "Network topology independent multi-agent dynamic optimal power flow for microgrids with distributed energy storage systems," *IEEE Trans. Smart Grid*, vol. 9, no. 4, pp. 3419-3429, Jul. 2018.

[16] X. Wu, C. Shen, and R. Iravani, "A distributed, cooperative frequency and voltage control for microgrids," *IEEE Transactions on Smart Grid*, vol. 9, no. 4, pp.2764-2776, 2018.

[17] C. Persis, E. Weitenberg, and F. Dörfler, "A power consensus algorithm for DC microgrids," *Automatica*, vol. 89, pp. 364–375, Mar. 2018.

[18] Y. Yang, S. C. Tan, and S. Y. R. Hui, "Mitigating distribution power loss of DC microgrids with DC electric springs," *IEEE Trans. Smart Grid*, vol. 9, no. 6, Nov. 2018.

[19] M. AlRashidi and M. El-Hawary, "A survey of particle swarm optimization applications in electric power systems," *IEEE Trans. Evol. Comput.*, vol. 13, no. 4, pp. 913-918, Aug. 2009.

[20] A. Selvakumar and K. Thanushkodi, "A new particle swarm optimization solution to nonconvex economic dispatch problems," *IEEE Trans. Power Syst.*, vol. 22, no. 1, pp. 42-51, Feb. 2007.

[21] A. K. Basu, A. Bhattacharya, S. Chowdhury, and S. P. Chowdhury, "Planned scheduling for economic power sharing in a CHP-based micro-Grid," *IEEE Trans. Power Syst.*, vol. 27, no.1, pp. 30-38, Feb. 2012.

[22] M. Hassan and M. Abido, "Optimal design of microgrids in autonomous and grid-connected modes using particle swarm optimization," *IEEE Trans. Power Electron.*, vol. 26, no. 3, pp. 755-769, Mar. 2011.

[23] M. Moghbel, M. A. S. Masoum, A. Fereidouni, and S. Deilami, "Optimal sizing, siting and operation of custom power devices with STATCOM and APLC Functions for real-time reactive power and network voltage quality control of smart grid," *IEEE Trans. Smart Grid.*, 2017, in press.

[24] H. Bevrani, F. Habibi, P. Babahajyani, M. Watanabe, and Y. Mitani, "Intelligent frequency control in an AC microgrid: online PSO-based fuzzy tuning approach," *IEEE Trans. Smart Grid*, vol. 3, no. 4, pp. 1935-1944, Dec. 2012.

[25] Z. Zhan, J. Zhang, O. Liu, and Y. Shi, "Orthogonal learning particle swarm optimization," *IEEE Trans. Evol. Comput.*, vol. 15, no. 6, pp. 832-847, Dec. 2011.

[26] X. Li and X. Yao, "Cooperatively coevolving particle swarms for large scale optimization," *IEEE Trans. Evol. Comput.*, vol. 16, no. 2, pp. 210-224, Apr. 2012.